



Thermo-elastic Analysis of Functionally Graded Thick- Walled Cylinder with Novel Temperature – Dependent Material Properties using Perturbation Technique

Hadi Mohammadi Hooyeh, Alireza Naddafoskouie*

Department of Solid Mechanics, Faculty of Mechanical Engineering, University of Eyvanekey, Garmsar, Iran

(Manuscript Received --- 18 Mar. 2018; Revised --- 20 May 2018; Accepted --- 04 July 2018)

Abstract

In this work, thermo – elastic analysis for functionally graded thick – walled cylinder with temperature - dependent material properties at steady condition is carried out. The length of cylinder is infinite and loading is consist of internal hydrostatic pressure and temperature gradient. All of physical and mechanical properties except the Poisson's ratio are considered as multiplied an exponential function of temperature and power function of radius. With these assumptions, the nonlinear differential equations for temperature distribution at cylindrical coordinate is obtained. Temperature distribution is achieved by solving this equation using classical perturbation method. With considering strain – displacement, stress – strain and equilibrium relations and temperature distribution that produced pervious, the constitutive differential equation for cylinder is obtained. By employing mechanical boundary condition the radial displacement is yield. With having radial displacement, stresses distribution along the thickness are achieved. The results of this work show that by increasing the order of temperature perturbation series the convergence at curves is occurred and also dimensionless radial stress decrease and other stresses with dimensionless radial displacement increase.

Keywords: Infinite thick – walled cylinder, nonlinear heat transfer, classical perturbation method, temperature-dependent properties, functionally graded material.

1- Introduction

Functionally graded materials (FGMs) are microscopically inhomogeneous in which the mechanical properties vary smoothly and continuously from one surface to the other [1-3]. FGMs are regarded as one of the most promising candidates for future advanced composites in many engineering sectors such as the aerospace, aircraft, automobile, and defense industries, and most recently the electronics and biomedical sectors [4-6]. All of these industries use piping systems and thick-walled cylinders. Many studies for thermal stresses of functionally graded cylinders are available in the literature.

Jabbaria et al. [7] represented a general analysis for one-dimensional steady-state thermal stresses in a hollow thick – walled FGM cylinder. They considered that the material properties, except Poisson's ratio, are assumed to depend on variable the radius and they are expressed as power function. Their results revealed that the magnitude of the radial stress is increased as the material parameter (m) is increased. Shao and Ma [8] studied thermo-mechanical analysis of functionally graded hollow circular cylinders subjected to mechanical loads and linearly increasing boundary temperature. They assumed that the thermo-mechanical properties of FGM to be temperature independent and vary

continuously in the radial direction of cylinder. They obtained time-dependent temperature and unsteady thermo-mechanical stresses by Laplace transform techniques and series solving method. Dai and Fu [9] presented exact solutions for stresses and perturbations of the magnetic field vector in FGM hollow cylinders using the infinitesimal theory of magneto-thermoelasticity. Their results illustrated that the inhomogeneity constant has a major effect on the magneto-thermoelastic stresses, a negative values yields compressive radial and circumferential stresses in the whole FGM hollow cylinder, while a positive values gives a contrary result. Axisymmetric displacements and stresses in functionally-graded hollow cylinders subjected to uniform internal pressure using plane elasticity theory and Complementary Functions method described by Tutuncu and Temel [10]. Shao and Wang [11] investigated analytical solutions of the three-dimensional temperature and thermo-elastic stress fields in the FGM cylindrical panel with finite length. They considered that the thermal and mechanical properties of the FGM to be temperature independent. Their results showed that the axial stress is larger than the radial stress and is smaller than the circumferential stress. Tutuncu [12] also obtained power series solutions for stresses and displacements in FG cylindrical vessels subjected to internal pressure alone using infinitesimal theory of elasticity. It is concluded from his results that a negative inhomogeneity constant would create a stress amplification effect. His study may be useful for specific applications to control the stress distribution. Mohammad and Mahboobeh Azadi [13] carried out nonlinear transient heat transfer and thermoelastic stress analyses of a thick-walled FGM cylinder with temperature - dependent materials using the Hermitian transfinite element method. The temperature distribution and the radial and circumferential stresses are investigated versus time, geometrical

parameters and index of power law in their research. Their research represented that by increasing of thickness, stresses decrease due to decreasing of temperature gradient. A novel method for thermoelastic analysis of a cylindrical vessel of FGMs presented by Peng and Li [14]. The thermal and thermoelastic parameters assumed to arbitrarily vary along the radial direction of the hollow cylinder in their work. They combined the boundary value problem with a thermoelastic problem and then converted to a Fredholm integral equation. Accordingly, by numerically solving the resulting equation, the distribution of the thermal stresses and radial displacement was obtained. They that appropriate gradient can make the distribution of thermal stresses more gentle in found the whole structure. Exact and approximate solutions of thermoelastic stresses in FG cylinders with power law and exponentially variations of material properties derived by Seifi [15]. He concluded that effects of high temperature on the stresses are more important than the high internal pressure. Exact thermoelastic analysis of FG anisotropic hollow cylinders with arbitrary material gradation provided by Vel [16]. He solved the differential equations of heat conduction and thermoelasticity using a power series solution technique. He found that the temperature, displacements and stresses are sensitive to the material gradation. Loghman and Parsa [17] analyzed the magneto-thermo-elastic response for a thick double-walled cylinder made from a FGM interlayer and a homogeneous outer layer. They showed that that under thermo-magneto-mechanical loading minimum effective stress distribution and the minimum radial displacement can be achieved by selecting an appropriate material parameter in the FGM layer. Ghorbanpour Arani and his research group [18] described electro-thermo-mechanical behavior of a radially polarized rotating functionally graded piezoelectric cylinder. They considered that the material

properties except Poisson's ratio and thermal conduction coefficient to be exponentially distributed along radius. It is concluded from their results that the inhomogeneity exponent plays a substantial role in radial and circumferential stress distributions. Thermo-electromechanical behavior of FG piezoelectric hollow cylinder under non-axisymmetric loads studied by Atrin et al. [19] Arefi and Rahimi [20] investigated the effect of nonhomogeneity and end supports on the thermo elastic behavior of a clamped-clamped FG cylinder under mechanical and thermal loads. They employed Hamilton principle and first order shear deformation theory (FSDT) for derivation of the principle differential equations. Their results showed that the absolute value of axial displacement of the cylinder decreases with increasing the non homogenous index. Thermal stresses analysis of a FG cylindrical shell under thermal shock based on differential quadrature method achieved by Zhang et al. [21] They illustrated that the thermal stresses could be alleviated by means of changing the volume fractions of the constituents. Thermo-elastic analysis of clamped-clamped thick FGM cylinders by using third-order shear deformation theory indicated by Gharooni et al. [22] They solved the set of nonhomogenous linear differential equations for the cylinder with clamped-clamped ends. It is observed from their results that using negative inhomogeneities in the cylinder causes small decreases under thermal load and considerable increase under mechanical load in radial displacements. Two – dimensional thermoelastic analysis of a FG cylinder for different functionalities by using the higher – order shear deformation theory presented by Arefi [23]. His results showed that the radial displacement decreases with increasing power law index due to an increase in the cylinder stiffness with increasing power law index.

Arefi and his research group [24] represented two-dimensional thermoelastic

analysis of FG cylindrical shell resting on the Pasternak foundation subjected to mechanical and thermal loads based on FSDT formulation. They used energy method and Euler equations for governing differential equations of system. They showed that by increasing the nonhomogeneity index both, radial and axial displacement decreases.

In all of previous studies that conducted on the FGM, a simply modeling for mechanical and physical changes properties was selected. These models were exponentially distributed or expressed by power function along the radius. In current work, we aimed to consider changes all physical and mechanical properties (except for Poisson's ratio) as a power function versus radius and a function of exponentially versus temperature. This action lead to nonlinear differential equation for heat transfer that by solving of it using perturbation technique we can use the temperature distribution at thermoelastic analysis.

2- Geometry, loading condition and assumptions

An infinitely long, functionally graded thick – walled hollow cylinder with inner radius a and outer radius b is considered. This cylinder is subjected to an internal hydrostatic pressure P_a and uniform temperature field with inner surface temperature T_a and outer temperature of T_b . One – dimensional and steady state heat conduction are selected for temperature distribution. Center cylindrical coordinates is on the center of the cylinder and axial symmetry in geometry and loading will be considered. Figure 1 shows the schematic view of the cylinder and its loading.

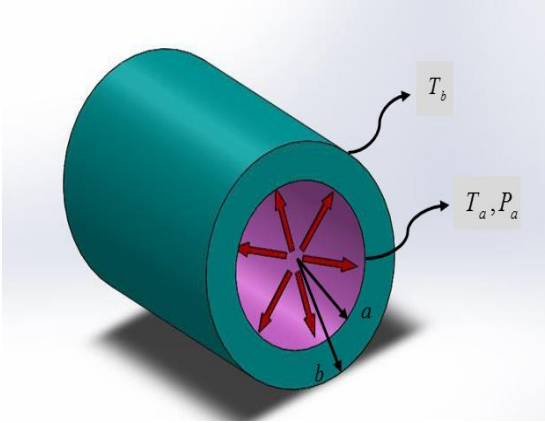


Figure 1. Schematic of FG cylinder under mechanical and thermal loads

3- Heat conduction problem

The heat conduction equation with regard to the above-mentioned assumptions and without any heat source is written in cylindrical coordinate as follow:

$$\frac{1}{r} \frac{\partial}{\partial r} \left(kr \frac{\partial \bar{T}}{\partial r} \right) = 0 \quad (1)$$

In which r, k and \bar{T} are radius, nominal heat conductivity coefficient and temperature distribution respectively.

It is assumed that the thermophysical and mechanical properties except the Poisson's ratio are considered as product of an exponential function of temperature and power function of radius. Furthermore, the nominal heat conductivity coefficient is assumed to depend on temperature as follow [25]:

$$k(r, \bar{T}) = k_0(r)k_1(\bar{T}) \quad (2)$$

The exponential function of temperature is assumed as follow form:

$$k_1(\bar{T}) = k_1 \exp(\beta^6(\bar{T} - T_a)) \quad (3)$$

The power function distribution in the radial direction considered as [25], [26]:

$$k_0(r) = k_0 r^m \quad (4)$$

Accordingly, for nominal heat conductivity coefficient can be written as follow:

$$k(r, \bar{T}) = k_2 r^m \exp(\beta^6(\bar{T} - T_a)) \quad (5)$$

$$k_2 = k_0 k_1$$

Where k_2, m, β are the physical constants characterizing the material behavior. By substituting Eq. (2) in to Eq. (1) we have:

$$\frac{d}{dr} (rk(r, \bar{T}) \frac{d\bar{T}}{dr}) = k(r, \bar{T}) \frac{d\bar{T}}{dr} + r \frac{dk(r, \bar{T})}{dr} \frac{d\bar{T}}{dr} + rk(r, \bar{T}) \frac{d^2 \bar{T}}{dr^2} = 0 \quad (6)$$

In which $\frac{dk(r, \bar{T})}{dr}$ is calculated using the product rule as follow:

$$\begin{aligned} \frac{dk(r, \bar{T})}{dr} &= \frac{d}{dr} (r^m) k_2 \exp(\beta^6(\bar{T} - T_a)) \\ &+ \frac{d}{dr} (\exp(\beta^6(\bar{T} - T_a))) k_2 r^m \\ &= mr^{m-1} k_2 \exp(\beta^6(\bar{T} - T_a)) + \end{aligned} \quad (7)$$

$$k_2 r^m \beta^6 \exp(\beta^6(\bar{T} - T_a)) \frac{d\bar{T}}{dr}$$

Substituting Eq. (7) in to Eq. (6) and then simplify, the following nonlinear differential equation of the second order is obtained:

$$\left(\frac{1+m}{r} \right) \frac{d\bar{T}}{dr} + \beta^6 \left(\frac{d\bar{T}}{dr} \right)^2 + \frac{d^2 \bar{T}}{dr^2} = 0 \quad (8)$$

3- 1- Perturbation technique

Perturbation technique is one of the most efficient approach to solving various boundary issues in elastic structures. This method as a means of approximate - analytically useful is employed to solve a large part of the nonlinear problems. According to the perturbation method, a complex nonlinear differential equation is divided to unlimited number of relatively simple equations (Perturbation equation). Accordingly, the solution of original equation is the summation of solving each Perturbation equations with the rising power of a small perturbation parameter as a coefficient is expressed. Therefore, the first few terms, represent the view of solving the problem. It is important at perturbation technique that the small perturbation parameter, select the appropriate. In using this method it is necessary that the small perturbation

parameter to be considered smaller than one. This method is used in continue.

By dividing Eq. (8) on m parameter we have:

$$\left(\frac{1}{m}+1\right)\frac{dT}{dr} + \frac{\beta^6}{m}\left(\frac{dT}{dr}\right)^2 + \frac{1}{m}\frac{d^2T}{dr^2} = 0 \tag{9}$$

The small ratio of $\frac{\beta^6}{m}$ is to appear in the nonlinear differential equation (9) that we can now define this ratio equal to small parameter ε . Therefore the Eq. (9) can be rewritten as follow:

$$\left(\frac{1}{m}+1\right)\frac{dT}{dr} + \varepsilon\left(\frac{dT}{dr}\right)^2 + \frac{1}{m}\frac{d^2T}{dr^2} = 0 \tag{10}$$

Perturbation theory leads to an expression for the desired solution in terms of a formal power series in some small parameter, known as a perturbation series, that quantifies the deviation from the exactly solvable problem. The leading term in this power series is the solution of the exactly solvable problem, while further terms describe the deviation in the solution, due to the deviation from the initial problem. Formally, we have for the approximation to the full solution \bar{T} , a series in the small parameter, like the ε following [27-30]:

$$\bar{T} = T_0\varepsilon^0 + \varepsilon^1T_1 + \varepsilon^2T_2 + \dots \tag{11}$$

In Eq. (11), T_0 would be the known solution to the exactly solvable initial problem and T_1, T_2, \dots represent the higher-order terms which may be found iteratively by some systematic procedure. For small ε these higher-order terms in the series become successively smaller. An approximate perturbation solution is obtained by truncating the series, usually by keeping only the first three terms, the second-order perturbation correction can be written as [30]:

$$\bar{T} \approx T_0\varepsilon^0 + \varepsilon^1T_1 + \varepsilon^2T_2 \tag{12}$$

By substituting Eq. (12) into Eq. (10) and grouping all terms with the same power of ε gives:

$$\begin{aligned} &\varepsilon^0\left(\frac{1}{m}\frac{d^2T_0}{dr^2} + \left(\frac{1}{r}\left(1 + \frac{1}{m}\right)\right)\frac{dT_0}{dr}\right) \\ &+ \varepsilon^1\left(\frac{1}{m}\frac{d^2T_1}{dr^2} + \left(\frac{1}{r}\left(1 + \frac{1}{m}\right)\right)\frac{dT_1}{dr} + \left(\frac{dT_0}{dr}\right)^2\right) \\ &+ \varepsilon^2\left(\frac{1}{m}\frac{d^2T_2}{dr^2} + \left(\frac{1}{r}\left(1 + \frac{1}{m}\right)\right)\frac{dT_2}{dr} + \left(\frac{dT_1}{dr}\right)^2\right) \\ &+ \varepsilon^3\left(\frac{dT_2}{dr}\right)^2 = 0 \end{aligned} \tag{13}$$

With setting zero coefficient of various powers of ε (the coefficient of ε^3 will be ignored) a set of differential equation can be obtained as follow:

$$\begin{aligned} O(\varepsilon^0): &\frac{1}{m}\frac{d^2T_0}{dr^2} + \left(\frac{1}{r}\left(1 + \frac{1}{m}\right)\right)\frac{dT_0}{dr} = 0 \\ O(\varepsilon^1): &\frac{1}{m}\frac{d^2T_1}{dr^2} + \left(\frac{1}{r}\left(1 + \frac{1}{m}\right)\right)\frac{dT_1}{dr} + \left(\frac{dT_0}{dr}\right)^2 = 0 \\ O(\varepsilon^2): &\frac{1}{m}\frac{d^2T_2}{dr^2} + \left(\frac{1}{r}\left(1 + \frac{1}{m}\right)\right)\frac{dT_2}{dr} + \left(\frac{dT_1}{dr}\right)^2 = 0 \end{aligned}$$

First, the $O(\varepsilon^0)$ problem is to be solved and then it results in higher-order approximation is used. The answer of $O(\varepsilon^0)$ problem can be achieved as:

$$T_0(r) = c_1 + \frac{c_2}{r^m} \tag{15}$$

c_1 and c_2 are the integration constants which can be determined by the following thermal boundary conditions:

$$T_0(r=a) = T_a \quad T_0(r=b) = T_b \tag{16}$$

Imposition of these boundary conditions onto the Eq. (15) gives the following relations for the integration constants c_1 and c_2 :

$$c_2 = \frac{(T_a - T_b)(r_b^m r_a^m)}{r_a^m - r_b^m}, \quad (17)$$

$$c_1 = \frac{T_a r_a^m - T_b r_b^m}{r_a^m - r_b^m}$$

By substituting Eq. (13) into the $O(\varepsilon^1)$ at Eq. (12), the differential equation for $O(\varepsilon^1)$ problem will be obtained as follow:

$$\frac{1}{m} \frac{d^2 T_1}{dr^2} + \frac{1}{r} \left(1 + \frac{1}{m}\right) \frac{dT_1}{dr} + \left(\frac{-mc_2}{r^{m+1}}\right)^2 = 0 \quad (18)$$

This is an inhomogeneous Cauchy–Euler ordinary differential equation whose general and particular solutions can be found as:

$$T_1(r) = \frac{c_3}{r^m} + c_4 - \frac{mc_2^2}{2r^{2m}} \quad (19)$$

The integration constants c_3 and c_4 can be achieved by applying thermal boundary conditions (16) to the solution (19) as:

$$c_3 = \frac{mc_2^2(r_a^{-2m} - r_b^{-2m}) + 2(T_a - T_b)}{2(r_a^{-m} - r_b^{-m})}$$

$$c_4 = \frac{(-mc_2^2 r_b^{-2m} - 2T_b)r_a^{-m}}{2(r_a^{-m} - r_b^{-m})} \quad (20)$$

$$+ \frac{r_b^{-m}(-mc_2^2 r_a^{-2m} - 2T_a)}{2(r_a^{-m} - r_b^{-m})}$$

As before, we substituting Eq. (19) into the $O(\varepsilon^2)$ at Eq. (12) and the $O(\varepsilon^2)$ differential equation will be represented as follow:

$$\frac{d^2 T_2}{dr^2} + \frac{1+m}{r} \frac{dT_2}{dr} + m \left(\frac{-mc_3}{r^{m+1}} + \frac{-m^3 c_2^2}{r^{m+1}}\right) = 0 \quad (21)$$

Eq. (21) is again an inhomogeneous Cauchy-Euler differential equation whose general solution is presented as the sum of the homogeneous solution and a particular solution as follow:

$$T_2(r) = -\frac{c_5}{r^m} + c_6 - \frac{1}{12} m^3 c_2^4 r^{-4m}$$

$$+ \frac{1}{3} m^2 c_2^2 c_3 r^{-3m} - \frac{1}{2} mc_3^2 r^{-2m} \quad (22)$$

Application of boundary conditions (16) to the general solution (22) yields the integration constants c_5 and c_6 as follow:

$$c_5 = \frac{m^3 c_2^4 (r_b^{-4m} - r_a^{-4m})}{12(r_b^{-m} - r_a^{-m})}$$

$$+ \frac{4m^2 c_2^2 c_3 (r_a^{-3m} - r_b^{-3m})}{12(r_b^{-m} - r_a^{-m})}$$

$$+ \frac{6mc_3^2 (r_b^{-2m} - r_a^{-2m}) + 12(T_b - T_a)}{12(r_b^{-m} - r_a^{-m})}$$

$$c_6 = \frac{m^3 c_2^4 r_a^{-m} (r_b^{-4m} - 4m^2 c_2^2 c_3 r_b^{-3m})}{12(r_a^{-m} - r_b^{-m})} \quad (23)$$

$$+ \frac{(6mc_3^2 r_b^{-2m} + 12T_b)m^3 c_2^4 r_a^{-m}}{12(r_a^{-m} - r_b^{-m})}$$

$$- \frac{m^3 c_2^4 r_b^{-m} (r_b^{-4m} - 4m^2 c_2^2 c_3 r_b^{-3m})}{12(r_a^{-m} - r_b^{-m})}$$

$$- \frac{(6mc_3^2 r_b^{-2m} + 12T_b)}{12(r_a^{-m} - r_b^{-m})}$$

Therefore, the temperature distributions at different orders of approximation can be obtained as follow:

$$\bar{T}_0(r) = \varepsilon^0 (c_1 + \frac{c_2}{r^m}) + O(\varepsilon^1)$$

$$\bar{T}_1(r) = \varepsilon^0 (c_1 + \frac{c_2}{r^m}) + \varepsilon^1 (\frac{c_3}{r^m} + c_4 - \frac{mc_2^2}{2r^{2m}}) + O(\varepsilon^2)$$

$$\bar{T}_2(r) = \varepsilon^0 (c_1 + \frac{c_2}{r^m}) \quad (24)$$

$$+ \varepsilon^1 (\frac{c_3}{r^m} + c_4 - \frac{mc_2^2}{2r^{2m}}) + \varepsilon^2 (-\frac{c_5}{r^m} + c_6 - \frac{1}{12} m^3 c_2^4 r^{-4m} + \frac{1}{3} m^2 c_2^2 c_3 r^{-3m} - \frac{1}{2} mc_3^2 r^{-2m}) + O(\varepsilon^3)$$

4- Thermoelastic analysis

4- 1- Stress – strain relations

The stress – strain relations at cylindrical coordinates system at general form can be written as follow [31]:

$$\begin{aligned}\varepsilon_r &= \frac{1}{E}(\sigma_r - \nu(\sigma_\theta + \sigma_z)) + \alpha_r \bar{T}(r) \\ \varepsilon_\theta &= \frac{1}{E}(\sigma_\theta - \nu(\sigma_r + \sigma_z)) + \alpha_\theta \bar{T}(r) \\ \varepsilon_z &= \frac{1}{E}(\sigma_z - \nu(\sigma_\theta + \sigma_r)) + \alpha_z \bar{T}(r) \\ \varepsilon_{r\theta} &= \frac{1}{2G} \sigma_{r\theta}, \varepsilon_{rz} = \frac{1}{2G} \sigma_{rz}, \varepsilon_{\theta z} = \frac{1}{2G} \sigma_{\theta z}\end{aligned}\quad (25)$$

In which r, θ and z denotes radial, circumferential and axial directions, respectively. σ_i and ε_i ($i = r, \theta, z$) are the stress and strain, ν and E are the Poisson's ratio and modulus elasticity, respectively. G is the young modulus and α_i ($i = r, \theta, z$) is the coefficient of thermal expansion that considered to be same at all coordinates. According to the assumptions, all shear strains and circumferential derivatives are zero and for plane strain conditions the axial stress is considered as follow:

$$\sigma_z = \nu(\sigma_r + \sigma_\theta) - E\alpha_z \bar{T}(r) \quad (26)$$

With substituting Eq. (26) into Eq. (25) and simplify, the stress – strain relations for functionally graded thick – walled cylinder at one – dimensional heat conduction are found as follow:

$$\begin{aligned}\sigma_r &= \bar{d}_1 \varepsilon_r + \bar{d}_2 \varepsilon_\theta - \bar{d}_3 \bar{T}(r) \\ \sigma_\theta &= \bar{d}_2 \varepsilon_r + \bar{d}_1 \varepsilon_\theta - \bar{d}_3 \bar{T}(r)\end{aligned}\quad (27)$$

The coefficients in Eq. (26) are in the power and exponential functions form and are defined as below:

$$\begin{aligned}\bar{d}_1 &= d_1 r^m \exp(\beta^6 (\bar{T} - T_a)) \\ d_1 &= \frac{E(1-\nu)}{(1+\nu)(1-2\nu)} \\ \bar{d}_2 &= d_2 r^m \exp(\beta^6 (\bar{T} - T_a)) \\ d_2 &= \frac{E(\nu)}{(1+\nu)(1-2\nu)} \\ \bar{d}_3 &= d_3 r^m \exp(\beta^6 (\bar{T} - T_a)) \\ d_3 &= d_1 \alpha_r + d_2 (\alpha_\theta + \alpha_z)\end{aligned}\quad (28)$$

4- 2- Strain – displacement relations

The stress – displacement relations at cylindrical coordinates system at general form can be obtained as follow [32]:

$$\begin{aligned}\varepsilon_r &= \frac{\partial u_r}{\partial r}, \varepsilon_\theta = \frac{u_r}{r} + \frac{1}{r} \frac{\partial u_\theta}{\partial \theta} \\ \varepsilon_\theta &= \frac{\partial u_z}{\partial z}, \varepsilon_{r\theta} = \frac{1}{r} \frac{\partial u_r}{\partial \theta} + \frac{\partial u_\theta}{\partial r} - \frac{u_\theta}{r} \\ \varepsilon_{rz} &= \frac{\partial u_r}{\partial z} + \frac{\partial u_z}{\partial r}, \varepsilon_{\theta z} = \frac{\partial u_\theta}{\partial z} + \frac{1}{r} \frac{\partial u_z}{\partial \theta}\end{aligned}\quad (29)$$

Where u_i ($i = r, \theta, z$) is the displacement vector. These relations with considering assumptions rewritten as below:

$$\varepsilon_r = \frac{\partial u_r}{\partial r}, \varepsilon_\theta = \frac{u_r}{r} \quad (30)$$

4- 3- Stress – displacement relations

Substituting Eq. (30) into Eq. (27), the stress – displacement relations yields as follow:

$$\begin{aligned}\sigma_r &= \bar{d}_1 \left(\frac{du_r}{dr} \right) + \bar{d}_2 \left(\frac{u_r}{r} \right) - \bar{d}_3 \bar{T}(r) \\ \sigma_\theta &= \bar{d}_2 \left(\frac{du_r}{dr} \right) + \bar{d}_1 \left(\frac{u_r}{r} \right) - \bar{d}_3 \bar{T}(r)\end{aligned}\quad (31)$$

4- 4- Equilibrium relations

The equilibrium equations of the hollow cylinder at general form are as follow [31], [32]:

$$\begin{aligned}\frac{\partial \sigma_r}{\partial r} + \frac{1}{r} \frac{\partial \tau_{r\theta}}{\partial \theta} + \frac{\partial \tau_{rz}}{\partial z} \\ + \frac{\sigma_r - \sigma_\theta}{r} + F_r = \rho \frac{\partial^2 u_r}{\partial t^2} \\ \frac{\partial \tau_{r\theta}}{\partial r} + \frac{1}{r} \frac{\partial \sigma_\theta}{\partial \theta} + \frac{\partial \tau_{\theta z}}{\partial z} \\ + \frac{2\tau_{r\theta}}{r} + F_\theta = \rho \frac{\partial^2 u_\theta}{\partial t^2} \\ \frac{\partial \tau_{rz}}{\partial r} + \frac{1}{r} \frac{\partial \tau_{r\theta}}{\partial \theta} + \frac{\partial \sigma_z}{\partial z} \\ + \frac{\tau_{rz}}{r} + F_z = \rho \frac{\partial^2 u_z}{\partial t^2}\end{aligned}\quad (32)$$

Where $F_i (i = r, \theta, z)$ are the body forces and ρ is the material density. The equilibrium equation of the FGM hollow cylinder, with considering previous assumptions and steady conditions in the absence of body forces, is expressed as:

$$\frac{\partial \sigma_r}{\partial r} + \frac{\sigma_r - \sigma_\theta}{r} = 0 \quad (33)$$

4- 5- Thermoelastic constitutive equation

By substituting the resulting temperature distribution from Eq. (24) into Eq. (31) and then into Eq. (33) the thermoelastic constitutive equation for FG thick – walled hollow cylinder with temperature – dependent material property is derived as follow:

$$\begin{aligned} & (r^2 d_1) \left(\frac{d^2 u_r}{dr^2} \right) + (r(m+1)d_1) \left(\frac{du_r}{dr} \right) \\ & + (md_2 - d_1)(u_r) \\ & - (rmd_3) \left((c_1 + c_2 r^{-m}) \right. \\ & \left. + \varepsilon \left(-\frac{1}{2} m c_2^2 r^{-2m} + c_3 r^{-m} + c_4 \right) \right. \\ & \left. + \varepsilon^2 \left(-\frac{1}{12} m^3 c_2^4 r^{-4m} + \frac{1}{3} m^2 c_2^2 c_3 r^{-3m} \right) \right. \\ & \left. - \frac{1}{2} m c_3^2 r^{-2m} + c_5 r^{-m} + c_6 \right) \\ & - (r^2 d_3) \left((-m c_2 r^{-m-1}) \right. \\ & \left. + \varepsilon \left(m^2 c_2^2 r^{-2m-1} - m c_3 r^{-m-1} \right) + \right. \\ & \left. \varepsilon^2 \left(\frac{1}{3} m^4 c_2^4 r^{-4m-1} \right. \right. \\ & \left. \left. - m^3 c_2^2 c_3 r^{-3m-1} \right. \right. \\ & \left. \left. + m^2 c_3^2 r^{-2m-1} \right. \right. \\ & \left. \left. - m c_5 r^{-m-1} \right) \right) = 0 \end{aligned} \quad (34)$$

This equation is the familiar Cauchy-Euler differential equation for radial displacement that characteristic equation for it is as follow:

$$\begin{aligned} & (d_1) \lambda^2 + (md_1) \lambda \\ & + (md_2 - d_1) = 0 \end{aligned} \quad (35)$$

The roots of the characteristic equation are:

$$\begin{aligned} \lambda_1 &= \frac{-md_1 + \sqrt{m^2 d_1^2 - 4m d_1 d_2 + 4d_1}}{2d_1} \\ \lambda_2 &= \frac{-md_1 - \sqrt{m^2 d_1^2 - 4m d_1 d_2 + 4d_1}}{2d_1} \end{aligned} \quad (36)$$

So, the general solution of the inhomogeneous equation (34) can be expressed as sum of particular solution and the general solution of the homogeneous one as below:

$$\begin{aligned} u(r) &= u_g(r) + u_p(r) = C_1 r^{\lambda_1} + C_2 r^{\lambda_2} + r g_1 + \\ & r^{-2m+1} g_2 + r^{-4m+1} g_3 - r^{-3m+1} g_4 \end{aligned} \quad (37)$$

In which:

$$\begin{aligned} g_1 &= \frac{m d_3 (c_1 + \varepsilon c_4 - c_6 \varepsilon^2)}{m(d_1 + d_2) + d_1} \\ g_2 &= \frac{1}{2} \frac{d_3 (\varepsilon m^2 c_2^2 + \varepsilon^2 m^2 c_3^2)}{(-2m+1)^2 d_1 + d_1(m+1)(-2m+1) + m d_2 - d_1} \\ g_3 &= \frac{1}{4} \frac{d_3 (\varepsilon^2 m^4 c_2^4)}{(-4m+1)^2 d_1 + d_1(m+1)(-4m+1) + m d_2 - d_1} \\ g_4 &= \frac{2}{3} \frac{d_3 (\varepsilon^2 m^3 c_3 c_2^2)}{(-3m+1)^2 d_1 + d_1(m+1)(-3m+1) + m d_2 - d_1} \end{aligned} \quad (38)$$

C_1 and C_2 are the integration constants which will be found as follow.

4- 5- Integration constants

By substituting radial displacement Eq. (37) into Eq. (31) the radial stress can be rewritten as:

$$\begin{aligned} \sigma_r = & d_1 r^m \exp(\beta^6 (T - T_a))(C_1 \lambda_1 r^{\lambda_1 - 1} \\ & + C_2 \lambda_2 r^{\lambda_2 - 1} \\ & + g_1 + (-2m + 1)r^{(-2m)} g_2 \\ & + (-4m + 1)r^{(-4m)} g_3 \\ & - (-3m + 1)r^{(-3m)} g_4) \\ & + d_2 r^m \exp(\beta^6 (T - T_a))(C_1 r^{\lambda_1 - 1} \\ & + C_2 r^{\lambda_2 - 1} + g_1 + r^{(-2m)} g_2 \\ & + r^{(-4m)} g_3 - r^{(-3m)} g_4) \\ & - d_3 r^m \exp(\beta^6 (T - T_a))(c_1 + c_2 r^{-m}) \quad (39) \\ & + \varepsilon \left(-\frac{1}{2} m c_2^2 r^{-2m} + c_3 r^{-m} + c_4 \right) \\ & + \varepsilon^2 \left(\begin{array}{l} -\frac{1}{12} m^3 c_2^4 r^{-4m} \\ +\frac{1}{3} m^2 c_2^2 c_3 r^{-3m} \\ -\frac{1}{2} m c_3^2 r^{-2m} \\ +c_5 r^{-m} + c_6 \end{array} \right) \end{aligned}$$

The thermoelastic problem is subjected to the following mechanical boundary conditions. The cylinder is loaded with internal hydrostatic pressure:

$$P(r = a) = -P_a \quad P(r = b) = 0 \quad (40)$$

Application of these boundary conditions to the radial stress (39) yields the following relations for the integration constants:

$$\begin{aligned} C_1 = & -\frac{1}{(a^{\lambda_2} b^{\lambda_1} - b^{\lambda_2} a^{\lambda_1})(\lambda_2 d_1 + d_2)} \\ & \times (12(-\frac{1}{2} b^{\lambda_1} (\varepsilon m (c_3^2 \varepsilon + c_2^2) d_3 \\ & - 4((m - \frac{1}{2}) d_1 - \frac{1}{2} d_2) g_2) a^{-2m+1} \\ & + \frac{1}{2} a^{\lambda_1} (\varepsilon m (c_3^2 \varepsilon + c_2^2) d_3 \\ & - 4((m - \frac{1}{2}) d_1 - \frac{1}{2} d_2) g_2) b^{-2m+1} \\ & - \frac{1}{12} b^{\lambda_1} (d_3 \varepsilon^2 m^3 c_2^4 \\ & - 48 g_3 ((m - \frac{1}{4}) d_1 - \frac{1}{4} d_2)) a^{-4m+1} \\ & + \frac{1}{3} b^{\lambda_1} (d_3 \varepsilon^2 m^2 c_2^2 c_3 \\ & - 9 g_4 ((m - \frac{1}{3}) d_1 - \frac{1}{3} d_2)) a^{-3m+1} \\ & + b^{\lambda_1} (-\exp(-\beta(T_a - T_a)) P_a \\ & + d_3 (c_5 \varepsilon^2 + c_3 \varepsilon + c_2) a^{-m+1} \\ & + \frac{1}{12} a^{\lambda_1} (d_3 \varepsilon^2 m^3 c_2^4 \\ & - 48 g_3 ((m - \frac{1}{4}) d_1 - \frac{1}{4} d_2)) b^{-4m+1} \\ & - \frac{1}{3} a^{\lambda_1} (d_3 \varepsilon^2 m^2 c_2^2 c_3 \\ & - 9 g_4 ((m - \frac{1}{3}) d_1 - \frac{1}{3} d_2)) b^{-3m+1} \\ & - a^{\lambda_1} (d_3 (c_5 \varepsilon^2 + c_3 \varepsilon + c_2) b^{-m+1} \\ & + (d_3 (c_6 \varepsilon^2 + c_4 \varepsilon + c_1) \\ & - g_1 (d_1 + d_2) (ab^{\lambda_1} - ba^{\lambda_1}))^2) \end{aligned}$$

$$\begin{aligned}
C_2 = & \frac{1}{12(a^{\lambda_2}b^{\lambda_1} - b^{\lambda_2}a^{\lambda_1})(\lambda_1d_1 + d_2)} \\
& \times (6(\varepsilon m(c_3^2\varepsilon + c_2^2)d_3 \\
& - 6a^{\lambda_2}(\varepsilon m(c_3^2\varepsilon + c_2^2)d_3 \\
& - 4((m - \frac{1}{2})d_1 - \frac{1}{2}d_2)g_2)b^{\lambda_2}a^{-2m+1} \\
& - 4((m - \frac{1}{2})d_1 - \frac{1}{2}d_2)g_2)b^{-2m+1} \\
& + b^{\lambda_2}(d_3\varepsilon^2m^3c_2^4 \\
& - 48g_3((m - \frac{1}{4})d_1 - \frac{1}{4}d_2))a^{-4m+1} \\
& - 4b^{\lambda_2}(d_3\varepsilon^2m^2c_2^2c_3 \\
& - 9g_4((m - \frac{1}{3})d_1 - \frac{1}{3}d_2))a^{-3m+1} \\
& - 12b^{\lambda_2}(-\exp(-\beta(T_a - T_0))P_a \\
& + d_3(c_5\varepsilon^2 + c_3\varepsilon + c_2)a^{-m+1} \\
& - a^{\lambda_2}(d_3\varepsilon^2m^3c_2^4 - 48g_3((m - \frac{1}{4})d_1 - \frac{1}{4}d_2))b^{-4m+1} \\
& + 4a^{\lambda_2}(d_3\varepsilon^2m^2c_2^2c_3 - 9g_4((m - \frac{1}{3})d_1 - \frac{1}{3}d_2))b^{-3m+1} \\
& + 12a^{\lambda_2}(+d_3(c_5\varepsilon^2 + c_3\varepsilon + c_2)b^{-m+1} \\
& - 12(d_3(c_6\varepsilon^2 + c_4\varepsilon + c_1) \\
& - g_1(d_1 + d_2)(ab^{\lambda_2} - ba^{\lambda_2}))^2)
\end{aligned} \quad (41)$$

With finding unknown constants the all stresses and radial displacement can be calculated. Also the Von Mises stress can be obtained as follow:

$$\sigma_{eff} = \frac{1}{\sqrt{2}} \left((\sigma_r - \sigma_\theta)^2 + (\sigma_r - \sigma_z)^2 + (\sigma_z - \sigma_\theta)^2 \right)^{\frac{1}{2}} \quad (42)$$

5- Numerical results and discussion

In the following numerical calculations, the mechanical and geometric properties for FGM cylinder are considered as [33-35]:

$$\begin{aligned}
E = 22(\text{GPa}) \quad \nu = 0.3 \\
\alpha = 1.2e-6(\frac{1}{^\circ\text{C}}) \\
P_a = 10(\text{MPa}) \quad \frac{b}{a} = 2
\end{aligned} \quad (43)$$

It should be noted that temperature values at inner and outer surfaces and other parameter is described after than any figure. For better analysis of results the dimensionless parameter are presented as follows:

$$\begin{aligned}
\sigma_i^* &= \left(\frac{\sigma_i}{P_a} \right) (i = r, \theta, z, eff) \\
r^* &= \left(\frac{r}{r_b} \right) \quad u^* = \left(\frac{u}{a} \right)
\end{aligned} \quad (44)$$

A distributed temperature field due to steady-state heat conduction for thick-walled FGM cylinder versus dimensionless radius with different orders of approximation illustrated in figure 2. It is shown from this figure that by increasing the orders of approximation from zeroth-order (i.e., linear problem) until the second-order solution the convergence of perturbation series is occurs. Also, it is observed easily that the thermal boundary conditions have been satisfied.

Figures 3 and 4 indicate the influence of physical constants characterizing the material behavior (m, β) on the temperature distribution (second – order). It is clear from figures 3 and 4 that by increasing the value of m and β the temperature distribution increases along the thickness of FGM cylinder.

Figure 5 represents the dimensionless radial stress distribution versus dimensionless radius with different orders of approximation. It is concluded that dimensionless radial stresses decreases with increasing orders of approximation. For this figure also convergence of perturbation series is obtained. Furthermore, it is compressive at the inner part of the cylinder which has to satisfy the internal pressure boundary condition.

Dimensionless circumferential and axial stresses along the thickness of cylinder with increasing the orders of approximation are demonstrated by Figures 6 and 7, respectively. It can be concluded from these figures that by

increasing dimensionless radius the dimensionless circumferential and axial stresses increases. It can be seen that maximum and minimum stresses happens at inner and outer surfaces, respectively. Figures 8 and 9 depicts the effects of increasing the orders of approximation on the dimensionless effective stresses and distribution of dimensionless radial displacement along the thickness of cylinder, respectively. It is shown that by increasing orders of approximation the dimensionless effective stress and dimensionless radial displacement increases. Also it is observed that maximum effective stress and radial displacement are at inner surface and it means that maximum damage occurs at in this surface.

The influence the influence of physical constants characterizing the material behavior (m, β) on the dimensionless effective stress are represented in figures 10 and 11. It is concluded from figure 10 that for constant value of β , by increasing the value of m the values of dimensionless effective stress at the inner layer to the middle layer of the cylinder has been reduced and the dimensionless effective stress values of the outer layer is added. Figure 11 show that by increasing the value of β , at constant value of m , the dimensionless effective stress decreases.

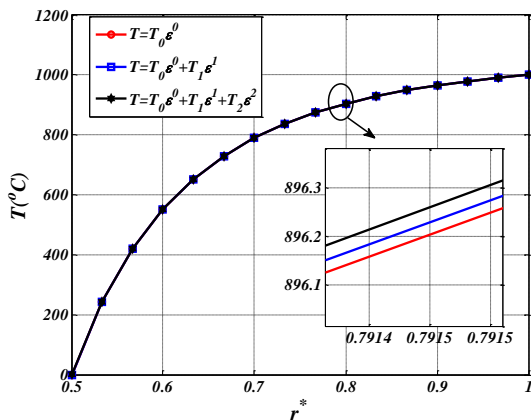


Figure2. Temperature distribution stress along the thickness of FGM cylinder with different orders of approximation $T_a = 0(^\circ C), T_b = 1000(^\circ C), m = 4, \beta = 0.09$

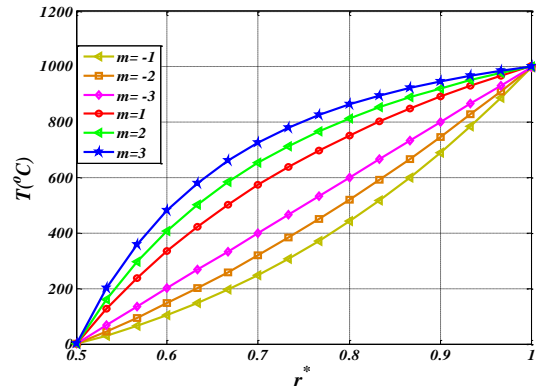


Figure3. Temperature distribution stress along the thickness of FGM cylinder with different value of $m T_a = 0(^\circ C), T_b = 1000(^\circ C), \beta = 0.09$

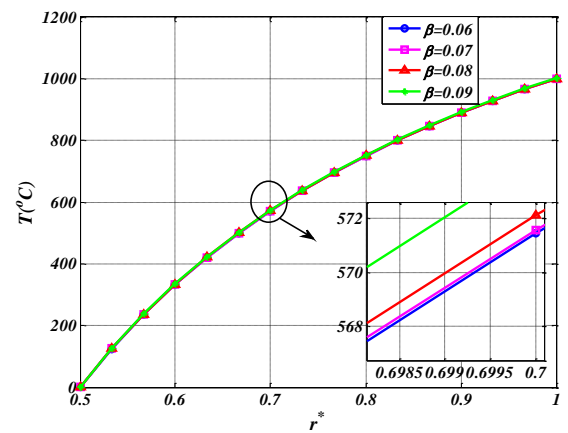


Figure4. Temperature distribution stress along the thickness of FGM cylinder with different value of $\beta T_a = 0(^\circ C), T_b = 1000(^\circ C), m = 1$

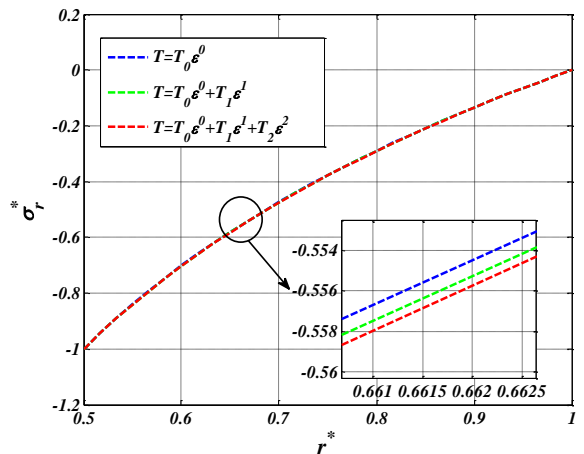


Figure5. Dimensionless radial stress along the thickness of FGM cylinder with different orders of approximation $T_a = 50(^\circ C), T_b = 150(^\circ C), m = 2, \beta = 0.2$

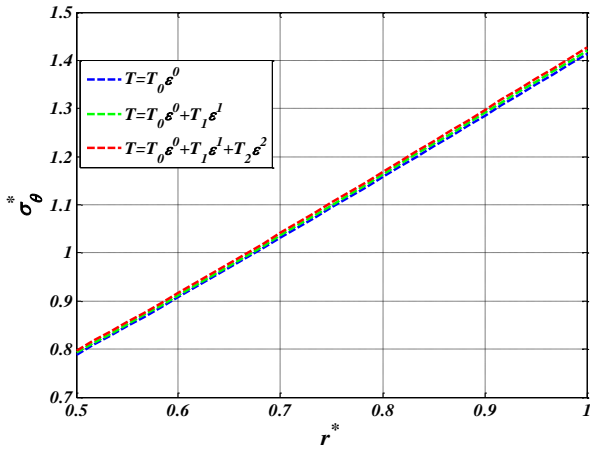


Figure6. Dimensionless circumferential stress along the thickness of FGM cylinder with different orders of approximation $T_a = 50(^{\circ}C), T_b = 150(^{\circ}C), m = 2, \beta = 0.2$

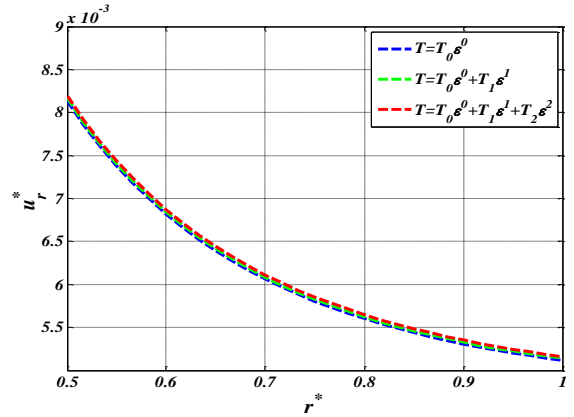


Figure9. Dimensionless radial stress along the thickness of FGM cylinder with different orders of approximation $T_a = 50(^{\circ}C), T_b = 150(^{\circ}C), m = 2, \beta = 0.2$

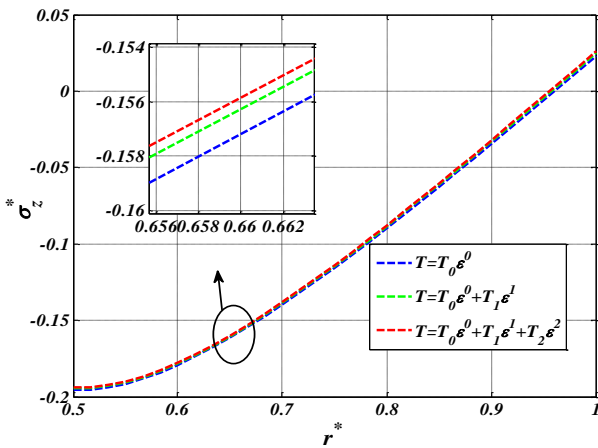


Figure7. Dimensionless axial stress along the thickness of FGM cylinder with different orders of approximation $T_a = 50(^{\circ}C), T_b = 150(^{\circ}C), m = 2, \beta = 0.2$

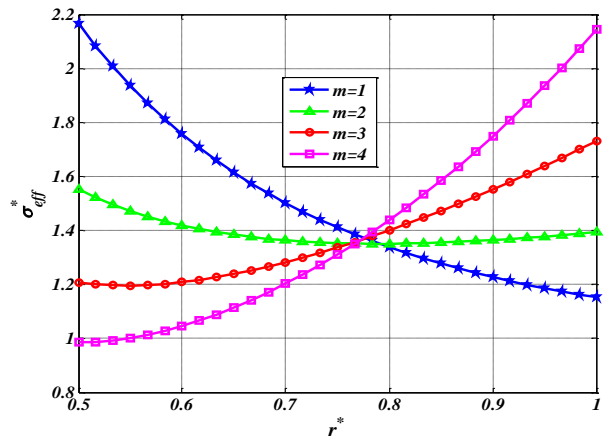


Figure10. Dimensionless effective stress along the thickness of FGM cylinder with different value of m $T_a = 50(^{\circ}C), T_b = 150(^{\circ}C), \beta = 0.01$

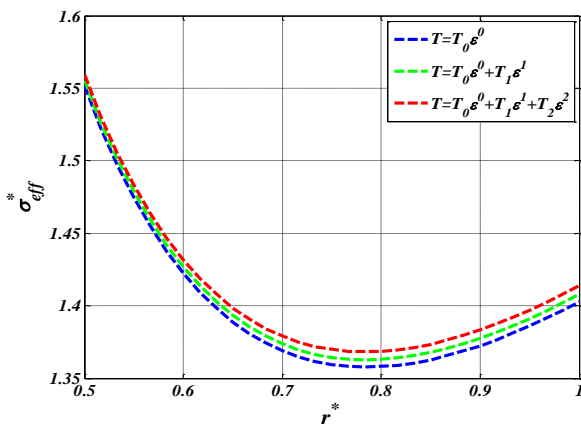


Figure8. Dimensionless effective stress along the thickness of FGM cylinder with different orders of approximation $T_a = 50(^{\circ}C), T_b = 150(^{\circ}C), m = 2, \beta = 0.2$

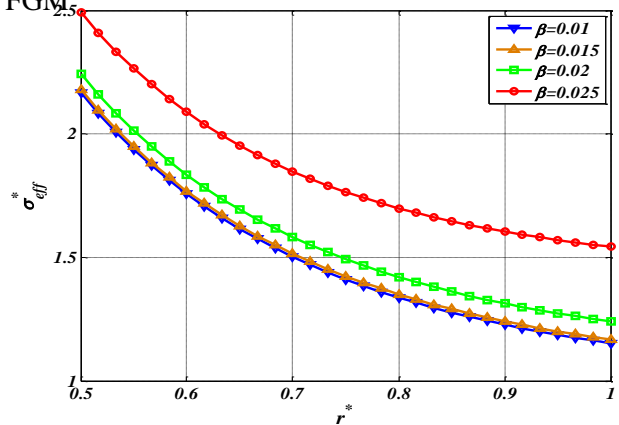


Figure10. Dimensionless effective stress along the thickness of FGM cylinder with different value of β $T_a = 50(^{\circ}C), T_b = 150(^{\circ}C), m = 1$

5- Conclusion

In this paper thermoelastic analysis of functionally graded thick –walled cylinder

with temperature dependent material property is investigated. This article represented a suitable approach for analysis material that their thermophysical and mechanical properties expect the Poisson's ratio are considered as product of an exponential function of temperature and power function of radius. For this purpose, perturbation technique is used to solving nonlinear differential equation for temperature distribution. This temperature distribution is employed at giving behavior of thermal stresses. The results of this article can be listed as follows:

- 1- By increasing the orders of approximation from zeroth-order (i.e., linear problem) until the second-order solution the convergence of perturbation series at all figures is occurs.
- 2- By increasing the value of m and β the temperature distribution increases along the thickness of FGM cylinder.
- 3- The dimensionless radial stresses decreases and dimensionless circumferential, axial and effective stresses and radial displacement increases with increasing orders of temperature approximation.
- 4- Maximum effective stress and radial displacement are located at inner surface. It means that maximum damage occurs at in this surface. The obtained results from this result can be used to design of cylindrical structures.
- 5- By increasing the value of m the dimensionless effective stress at the inner layer to the middle layer of the cylinder has been reduced and the dimensionless effective stress at the outer layer increases. Also by increasing the value of β the dimensionless effective stress decreases.

References:

- [1] S. Suresh, and A. Mortensen, *Fundamentals of functionally graded materials*, Barnes and Noble Publications, 1998.
- [2] M.Yamanouchi, and M. Koizumi, *Functionally gradient materials*. Proceeding of the first international symposium on functionally graded materials, Sendai, Japan, 1991.
- [3] M.M. Najafizadeh, and H.R. Heydari, An exact solution for buckling of functionally graded circular plates based on higher order shear deformation plate theory under uniform radial compression, *Int. J. Mech. Sci.*, vol. 50, pp. 603–612, 2008.
- [4] H.J. Xiang, and J. Yang, Free and forced vibration of a laminated FGM Timoshenko beam of variable thickness under heat conduction, *Compos. Part B (Eng)*, vol. 39, pp. 292–303, 2008.
- [5] R. Ansari, and M. Darvizeh, Prediction of dynamic behaviour of FGM shells under arbitrary boundary conditions, *Compos. Struct.*, vol. 85, pp. 284–292, 2008.
- [6] A. Allahverdizadeh, M.H. Naei, and M. Nikkhah Bahrami, Vibration amplitude and thermal effects on the nonlinear behavior of thin circular functionally graded plates, *Int. J. Mech. Sci.*, vol. 50, pp. 445–454, 2008.
- [8] M. Jabbaria, S. Sohrabpourb, and M.R. Eslamic, Mechanical and thermal stresses in a functionally graded hollow cylinder due to radially symmetric loads, *Int. J. Pressure Vessels Piping*, vol. 79, pp. 493–497, 2002.
- [9] Z.S. Shao, and G.W. Ma, Thermo-mechanical stresses in functionally graded circular hollow cylinder with linearly increasing boundary temperature, *Compos. Struct.*, vol.83 pp. 259–265, 2008.
- [10] H.L. Dai, and Y.M. Fu, Magneto-thermoelastic interactions in hollow structures of functionally graded material subjected to mechanical loads, *Int. J. Pressure Vessels Piping* vol. 84 pp. 132–138, 2007.

- [11] N.Tutuncu, and B. Temel, A novel approach to stress analysis of pressurized FGM cylinders, disks and spheres, *Compos. Struct.*, vol. 91, pp. 385–390, 2009.
- [12] Z. Shao, T.J. Wang, Three-dimensional solutions for the stress fields in functionally graded cylindrical panel with finite length and subjected to thermal/mechanical loads, *Int. J. Solids. Struct.*, vol.43, pp. 3856-3874, 2006.
- [13] N. Tutuncu, Stresses in thick-walled FGM cylinders with exponentially-varying properties, *Eng. Struct.*, vol.29, pp.2032-2035, 2007.
- [14] M. Azadi, and M. Azadi, Nonlinear transient heat transfer and thermoelastic analysis of thick-walled FGM cylinder with temperature-dependent material properties using Hermitian transfinite element, *J. Mech. Sci Tech.*, vol. 23, pp. 2635-2644, 2009.
- [15] X.L. Peng, and X.F. Li, Thermoelastic analysis of a cylindrical vessel of functionally graded materials, *Int. J. Pressure Vessels Piping*, vol. 87 pp. 203 - 210, 2010.
- [16] R. Seifi, Exact and approximate solutions of thermoelastic stresses in functionally graded cylinders, *J. Thermal Stresses*, vol. 38, pp. 1163–1182, 2015.
- [17] S.S.Vel, Exact thermoelastic analysis of functionally graded anisotropic hollow cylinders with arbitrary material gradation, *Mech. Adv. Mater. Struct.*, vol. 18, pp.14–31, 2011.
- [18] A. Loghman, and H. Parsa, Exact solution for magneto-thermo-elastic behaviour of double-walled cylinder made of an inner FGM and an outer homogeneous layer, *Int. J. Mech. Sci.*, vol. 88, pp. 93-99, 2014.
- [19] A. Ghorbanpour Arani, A. Loghman, A. Abdollahitaheri, and V. Atabakhshian, Electrothermomechanical behavior of a radially polarized rotating functionally graded piezoelectric cylinder, *J. Mech. Mater. Struct.*, vol.6, pp.869-882, 2011.
- [19] A. Atrin, J. Jafari Fesharaki, and S. H. Nourbakhsh, Thermo-electromechanical behavior of functionally graded piezoelectric hollow cylinder under non-axisymmetric loads, *Appl. Math. Mech. Engl. Ed.*, vol. 35, pp. 939–954, 2015.
- [20] M. Arefi, and G.H. Rahimi, The effect of nonhomogeneity and end supports on the thermo elastic behavior of a clamped-clamped FG cylinder under mechanical and thermal loads, *Int. J. Press Vessels Piping*, vol. 96, pp. 30-37, 2012.
- [21] J.H. Zhang, G.Z. Li, S.R. Li, and Y.B. Ma, DQM-based thermal stresses analysis of a functionally graded cylindrical shell under thermal shock, *J. Thermal Stresses*, vol. 38, pp. 959–982, 2015.
- [22] H. Gharooni, M. Ghannad, and M.Z.Nejad, Thermo-elastic analysis of clamped-clamped thick FGM cylinders by using third-order shear deformation theory, *Latin American Journal of Solids and Structures*, vol. 13, pp. 750-774, 2016.
- [23] M. Arefi, Two – dimensional thermoelastic analysis of a FG cylinder for different functionalities by using the higher – order shear deformation theory, *J. Appl. Mech. Tech. Phys*, vol. 56, pp. 494–501, 2015.
- [24] M. Arefi , A.R. Abbasi, and M.R.Vaziri Sereshk, Two-dimensional thermoelastic analysis of FG cylindrical shell resting on the Pasternak foundation subjected to mechanical and thermal loads based on FSDT formulation, *J. Thermal stresses*, vol. 39, pp. 554-570, 2016.
- [25] M. Arefi, Nonlinear thermal analysis of a functionally graded hollow cylinder with temperature variable material properties, *J. Appl. Mech. Tech. Phys.*, vol. 56, pp. 267-273, 2015.
- [26] A. loghman, and M. Moradi, The analysis of time-dependent creep in FGPM thick walled sphere under electro-magneto-thermo-mechanical loadings, *Mech. Time-Dependent Materials*, vol. 17, pp. 315–329, 2013.
- [27] A.M. Wazwaz, *Partial differential equations and solitary Waves theory*, Nonlinear Physical Science, Springer, 2009.

- [28] A. Sadighi, and D.D. Ganji, Exact solutions of Laplace equation by homotopy-perturbation and Adomian decomposition methods, *Phys. Lett. A.*, vol. 367, pp. 83-87, 2007.
- [29] R. Vatankhah, M.H. Kahrobaian, A. Alasty, and M.T. Ahmadian, Nonlinear forced vibration of strain gradient microbeams, *Appl. Math. Model.*, vol. 37, pp. 8363–8382, 2013.
- [30] A. Moosaie, Axisymmetric steady temperature field in FGM cylindrical shells with temperature-dependent heat conductivity and arbitrary linear boundary conditions, *Arch. Mech.*, vol. 67, pp. 233–251, 2015.
- [31] A.C., Ugural, and S.K., Fenster, *Advanced strength and applied elasticity*, New Jersey Institute of Technology, 2003.
- [31] A. Alibeigloo, A.M. Kani, and M.H. Pashaei, Elasticity solution for the free vibration analysis of functionally graded cylindrical shell bonded to thin piezoelectric layers, *Int. J. Pressure Vessels Piping*, vol. 89, pp. 98-111, 2012.
- [32] A. Loghman, S.M.A. Aleayoub, and M. Hasani Sadi, Time-dependent magnetothermoelastic creep modeling of FGM spheres using method of successive elastic solution, *Appl. Math. Model.*, vol. 36, pp. 836-845, 2012.
- [33] J. Jafari Fesharaki, A. Loghman, M. Yazdipoor, and S. Golabi, Semi-analytical solution of time-dependent thermomechanical creep behavior of FGM hollow spheres, *Mech. Time-Dependent Materials*, vol. 18, pp. 41–53, 2014.
- [34] A. Loghman, A. Ghorbanpour Arani, S. Amir, and A. Vajedi, Magnetothermoelastic creep analysis of functionally graded cylinders, *Int. J. Pressure Vessels Piping*, vol. 87, pp. 389-395, 2010.

